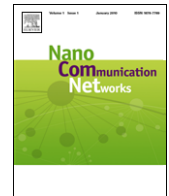




ELSEVIER

Contents lists available at ScienceDirect

## Nano Communication Networks

journal homepage: [www.elsevier.com/locate/nanocomnet](http://www.elsevier.com/locate/nanocomnet)

## Deterministic capacity of information flow in molecular nanonetworks

Baris Atakan\*, Ozgur B. Akan

*Next generation Wireless Communications Laboratory, Department of Electrical and Electronics Engineering, Middle East Technical University, 06531, Ankara, Turkey*

## ARTICLE INFO

*Article history:*

Received 2 March 2010

Accepted 15 March 2010

Available online xxxx

*Keywords:*

Molecular communication

Nanoscale communication

Information flow in nanonetworks

Molecular communication channel capacity

## ABSTRACT

Molecular communication enables nanomachines to exchange information with each other by emitting molecules to their surrounding environment. Molecular nanonetworks are envisioned as a number of nanomachines that are deployed in an environment to share specific molecular information such as odor, flavor, or any chemical state. In this paper, using the stochastic model of molecular reactions in biochemical systems, a realistic channel model is first introduced for molecular communication. Then, based on the realistic channel model, we introduce a deterministic capacity expression for point-to-point, broadcast, and multiple-access molecular channels. We also investigate information flow capacity in a molecular nanonetwork for the realization of efficient communication and networking techniques for frontier nanonetwork applications. The results reveal that molecular point-to-point, broadcast, and multiple-access channels are feasible with a satisfactorily high molecular communication rate, which allows molecular information flow in nanonetworks. Furthermore, the derived molecular channel model with input-dependent noise term also reveals that unlike a traditional Gaussian communication channel, achievable capacity is affected by both lower and upper bounds of the channel input in molecular communication channels.

© 2010 Elsevier Ltd. All rights reserved.

## 1. Introduction

Nanotechnology envisages the practical realization of very low-end nanomachines that have tiny components to accomplish a simple specific task such as communication, computation, and sensing in a scale ranging from 1 to 100 nanometers. For example, programmable molecular nanomachines that are formed by precisely organized molecule and atom configurations are envisioned to accomplish specific tasks. These machines are also designed with significant abilities to physically configure themselves based on the task requirements or sensing information. They are also considered as part of potential solution approaches for pollution, scarce food resources, and cellular repair [1].

At the same time, existing nanoscale biological entities such as functional living cell components, bacterium, and viruses are also viewed as nanomachines. The realization of such nanomachines has also been worked on by a large set of biochemical methods for many years. For example, biochemists are already tackling the production of functional cell components such as ribosomes that can be used for the synthesis of beneficial proteins. Moreover, bacteria are also genetically programmed to generate principle vital components ranging from human growth hormone to beneficial enzymes for cheese production. Moreover, by mixing viral proteins with a special DNA in a test tube, it might be possible to generate a kind of T<sub>4</sub> phage virus that sticks to a bacterium and injects viral DNA to program the bacterium for the generation of excessive viral DNA and infections [1].

Doubtlessly, a network of communicating nanomachines can also be programmed to share nanoscale information over a nanonetwork so as to fulfill more complex tasks such as collaborative drug delivery, health monitoring, and biological or chemical attack detection [2,3]. In

\* Corresponding author. Tel.: +90 312 210 4584; fax: +90 312 210 2304.

E-mail addresses: [atakan@eee.metu.edu.tr](mailto:atakan@eee.metu.edu.tr) (B. Atakan),  
[akan@eee.metu.edu.tr](mailto:akan@eee.metu.edu.tr) (O.B. Akan).



in an infinitesimally small electrochemical pulse to allow RN to infer the delivery of a molecular information. A reaction between a molecule and receptor occurs if the collision point of the molecule overlaps with the location of a receptor.

Here, we also define a *virtual reception volume* (VRV), center of which is the location of RN, and all of the reactions among the molecules and receptors take place in VRV as in Fig. 1. VRV is selected as a sufficiently small volume that surrounds RN to exactly follow the stochastic dynamics of the reactions among molecules and receptors. The size of VRV, i.e.,  $v_r$  is assumed to be constant and greater than the volume of RN. The molecules that collide and react with the receptors are not grasped and permanently enclosed by RN. After the reaction, the molecule continues its free diffusion in the environment.

We assume that TN emits the molecules  $L$  with an initial concentration<sup>1</sup>  $x$  to the medium at time  $t_0$ . Note that  $x$  is the input to the molecular channel derived below. The emitted molecules start to diffuse in the medium and at time  $t$ , the concentration of molecules in VRV, i.e.,  $x_t$  can be given as [3]

$$x_t = \frac{x}{(4\pi Dt)^{3/2}} e^{-\frac{d^2}{4Dt}}, \quad (1)$$

where  $D$  is the translational diffusion coefficient for molecules  $L$  and  $d$  is the distance between TN and RN. Hence, at time  $t$ , the number of molecules that might be available and chemically react with the receptors in VRV is  $x_t$ .

There are mainly two approaches to mathematically characterize the temporal evolution of spatially homogeneous chemically reacting systems [13]. The first approach, called deterministic approach, identifies time evolution as a predictable process by a set of coupled ordinary differential equations also called reaction-rate equations. The second is the stochastic approach that considers time evolution as a random-walk process which is characterized by a single differential (or difference) equation called the master equation. The deterministic approach considers the time evolution of a chemically reacting system as continuous and deterministic. However, the evolution is not a continuous process since the number of molecules due to chemical reactions changes by discrete amounts. Furthermore, the evolution is evidently a non-deterministic process such that it is impossible to predict the exact molecular population levels during a time interval unless the precise positions and velocities of all molecules are considered [11]. Here, in order to devise a realistic channel model in molecular communication, we follow a stochastic approach introduced for describing the stochastic simulation of coupled chemical reactions [11]. The number of reactions occurring in VRV during a time interval is actually a random variable since it is not possible to track locations and positions of all molecules. Here, our aim is to

describe the evolution of the number of reactions within a time interval. For this aim, it can be possible to define a probability, i.e.,  $a(x_t)dt$ , that one reaction occurs between a molecule and receptor in the next infinitesimally small time interval  $[t, t + dt)$ .  $a(x_t)$  is commonly referred to as propensity function in the stochastic analysis of chemically reacting systems and also provides the logical basis for stochastic chemical kinetics in stochastic simulation algorithms [14].  $a(x_t)$  also has a special mathematical form [15] as

$$a(x_t) = \eta\gamma, \quad (2)$$

where  $\eta$  is the specific probability rate constant for the molecular reaction among the molecules and receptors in VRV, and  $\gamma$  is the number of distinct combinations of molecule and receptor pairs available in VRV.  $\eta dt$  also gives the probability that a randomly chosen molecule and receptor pair reacts during the next  $dt$ .  $\eta dt$  can be computed<sup>2</sup> using the average velocity of molecules, the size of VRV, and the volume of the molecules and RN [11]. Note that  $\gamma$  can be directly obtained by inspecting the reaction  $L + R \rightarrow \text{electrochemical pulse} + L + R$ . Clearly, since there are  $rx_t$  distinct combinations of molecules and receptors for such a reaction,  $\gamma$  can be set as  $\gamma = rx_t$ , where  $r$  is the concentration of receptors  $R$  on RN. Substituting  $\eta$ ,  $r$ , and  $x_t$  given in (1) into (2),  $a(x_t)$  can be also written as

$$a(x_t) = \left[ \frac{\eta r e^{-\frac{d^2}{4Dt}}}{(4\pi Dt)^{3/2}} \right] x. \quad (3)$$

Using  $a(x_t)$ , we establish the stochastic dynamics of reactions in VRV as follows. Let  $y(t, \tau)$  be the number of reactions that occur within the time interval  $[t, t + \tau]$ .  $y(t, \tau)$  is clearly a random variable and its computation for an arbitrary  $\tau > 0$  is nontrivial and necessitates the solution of a stochastic chemical master equation that does not always have a solution. However, it can be possible to obtain an easier and excellent approximation for  $y(t, \tau)$  if the following conditions can be satisfied [14]:

- (1)  $\tau$  should be small enough such that during the interval  $[t, t + \tau]$ , the changes in the system state will be very slight, that is,

$$a(x_t) \cong a(x_{t+t'}) \quad \forall t' \in [t, t + \tau]. \quad (4)$$

If (4) is satisfied, the rate of reactions does not significantly change in the interval  $[t, t + \tau]$ . With this condition, all reaction events within the interval  $[t, t + \tau]$  can be clearly independent with each other. Hence,  $y(t, \tau)$  is simply a Poisson random variable with the rate  $\lambda = a(x_t)\tau$  [14].

- (2)  $\tau$  should be large enough such that the expected number of reactions in the interval  $[t, t + \tau]$  should be much larger than 1, that is,

$$a(x_t)\tau \gg 1. \quad (5)$$

<sup>1</sup> Since concentration of molecules ( $\mu\text{mol/l}$ ) can be converted to number of molecules by multiplying Avagadro constant ( $6.02 \times 10^{23}$ ), we interchangeably use the number of molecules for the concentration of molecules.

<sup>2</sup> The computation of  $\eta$  is beyond the scope of this paper. In the numerical analysis of this paper, we select  $\eta$  as a physically feasible value and only observe its effect on the molecular communication capacity.

If (5) is satisfied, the Poisson random variable  $y(t + \tau)$  can be approximated by the corresponding normal random variable  $N(\lambda, \lambda)$ , that is,  $N(a(x_t)\tau, a(x_t)\tau)$  [14]. In order to satisfy (5),  $x$  must be greater than a lower bound, i.e.,  $x_t$ , since  $a(x_t)$  is a strictly increasing function of  $x$  as seen in (3). Thus,  $x \geq x_t$  must be satisfied in order to obtain a coherent normal distribution approximation for  $y$ . The normal random variable  $y$  given as  $N(a(x_t)\tau, a(x_t)\tau)$  also can be simplified as a standard normal random variable based on

$$N(\mu, \sigma^2) = \mu + \sigma N(0, 1). \quad (6)$$

By setting  $\mu = a(x_t)\tau$  and  $\sigma = [a(x_t)\tau]^{\frac{1}{2}}$  and substituting into (6),  $y(t, \tau)$  can be expressed as

$$y(t, \tau) = a(x_t)\tau + [a(x_t)\tau]^{\frac{1}{2}}z, \quad (7)$$

where  $z$  is the standard normal random variable  $N(0, 1)$ . Using the derivation of  $x_t$  and  $a(x_t)$  given above and substituting them into (7),  $y(t, \tau)$  can be rewritten as

$$y(t, \tau) = \left[ \frac{\eta r \tau e^{-\frac{r^2}{4Dt}}}{(4\pi Dt)^{3/2}} \right] x + \left[ \frac{\eta r \tau e^{-\frac{r^2}{4Dt}}}{(4\pi Dt)^{3/2}} x \right]^{\frac{1}{2}} z. \quad (8)$$

Here, in order to simplify the capacity analysis of the molecular channels in the following section, we also normalize the concentration of emitted molecules ( $x$ ) over the interval  $[0, 1]$  by using an upper bound for  $x$ . This is similar to the transmission power constraint in traditional communication channels. Hence, by normalizing  $x$  over the interval  $[0, 1]$ , (8) can be given as

$$y(t, \tau) = \left[ \frac{\eta r \tau e^{-\frac{r^2}{4Dt}} x_u}{(4\pi Dt)^{3/2}} \right] \frac{x}{x_u} + \left[ \frac{\eta r \tau e^{-\frac{r^2}{4Dt}} x_u}{(4\pi Dt)^{3/2}} \frac{x}{x_u} \right]^{\frac{1}{2}} z, \quad (9)$$

where  $x_u$  is the upper bound for  $x$ . (9) can be also simplified as

$$y(t, \tau) = h(t, \tau)\bar{x} + [h(t, \tau)\bar{x}]^{\frac{1}{2}}z, \quad (10)$$

where  $\bar{x}$  denotes the normalized  $x$ , i.e.,  $\bar{x} = \frac{x}{x_u}$ , and  $h(t, \tau)$  is defined as

$$h(t, \tau) = \frac{\eta r \tau e^{-\frac{r^2}{4Dt}} x_u}{(4\pi Dt)^{3/2}}. \quad (11)$$

Clearly, (10) forms a channel model for molecular communication and is similar with a Gaussian channel model in which  $\bar{x}$  is the channel input,  $y(t, \tau)$  is the channel output,  $h(t, \tau)$  is the channel gain and  $[h(t, \tau)\bar{x}]^{\frac{1}{2}}z$  is the noise term that includes a white noise term  $z$  and an input-dependent term  $[h(t, \tau)\bar{x}]^{\frac{1}{2}}$ . Since the channel gain  $h(t, \tau)$  is a function of time, the molecular communication channel has time-varying characteristics. However, based on the assumption that  $h(t, \tau)$  slightly changes within each  $[t, t + \tau]$ , the characteristics of the molecular communication channel can be investigated throughout each consecutive interval of  $\tau$ . Hence, in the following sections, capacity and numerical analyses of the molecular channel given in (10) are performed within the consecutive intervals of  $\tau$ . Note that, hereafter for ease of illustration, we denote the normalized channel input as  $x$  instead of  $\bar{x}$ . Next, using the channel model derived in this section, we investigate the achievable molecular capacities for molecular communication channels.

### 3. Deterministic analysis of molecular nanonetworks

In this section, based on the deterministic analysis of wireless networks [16] and the molecular channel model given in (10), we first introduce a deterministic capacity analysis and derive a capacity expression for point-to-point, broadcast, and multiple-access molecular channels. Then, based on these analyses and capacity expressions, we investigate information flow in a molecular nanonetwork and discuss the feasibility of networking techniques that enable the predicted capacity levels in molecular nanonetworks.

#### 3.1. Point-to-point molecular channel

In the point-to-point molecular channel (see Fig. 2), a TN and RN exist in the system and TN emits molecules with concentration  $x$  to its surroundings in a single puff as a point source at time  $t = t_0$ . Some of the emitted molecules diffuse toward RN and collide with the receptors on its surface. Each of the collided molecules is assumed to cause molecular information delivery to RN. During a sufficiently long  $\tau$ , the concentration of the delivered molecules, i.e.,  $y(t, \tau)$ , can be given as in (10). Using the binary expansion of  $x$  and  $z$ , (10) can be rewritten as follows [16]

$$y(t, \tau) = 2^{\log h(t, \tau)} \sum_{i=1}^{\infty} x(i)2^{-i} + 2^{\frac{1}{2} \log h(t, \tau)x} \sum_{i=-\infty}^{\infty} z(i)2^{-i}, \quad (12)$$

where  $\log(\cdot)$  is used with base 2. In order to simplify the effect of the noise, setting the peak power of the white noise term  $z$  as 1, (12) can be approximated as

$$y(t, \tau) \approx 2^{n(t, \tau)} \sum_{i=1}^{\infty} x(i)2^{-i} + 2^{k(t, \tau)} \sum_{i=1}^{\infty} z(i)2^{-i}, \quad (13)$$

where  $\lceil \log h(t, \tau) \rceil = n(t, \tau)$  and  $\lceil \frac{1}{2} \log h(t, \tau)x \rceil = k(t, \tau)$ . By further simplifying, (13) can be also expressed as

$$y(t, \tau) \approx 2^{n(t, \tau)} \sum_{i=1}^{n(t, \tau) - k(t, \tau)} x(i)2^{-i} + 2^{k(t, \tau)} \sum_{i=1}^{\infty} [x(i + n(t, \tau) - k(t, \tau)) + z(i)]2^{-i}. \quad (14)$$

Ignoring the carry bit from the second term  $\sum_{i=1}^{\infty} [x(i + n(t, \tau) - k(t, \tau)) + z(i)]2^{-i}$ , (14) approximately represents the point-to-point molecular channel given in (12). As seen in (14), RN receives  $[n(t, \tau) - k(t, \tau)]$  most significant bits of the input  $x$  without any noise while the rest are not seen at all due to the noise [16]. Here, the concept of bit is not the same with traditional digital communication since we do not consider any digital coding mechanism for the transmission of molecular information. If  $[n(t, \tau) - k(t, \tau)]$  most significant bits of the channel input are received by RN in the interval  $[t, t + \tau]$ , this means the reception of a number of molecules which is equal to the decimal

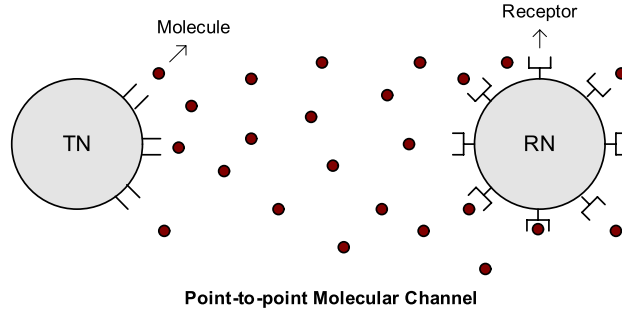


Fig. 2. Point-to-point molecular channel in which a single TN communicates with a single RN by emitting molecules.

equivalent of  $[n(t, \tau) - k(t, \tau)]$  most significant bits in the binary version of the channel input  $x$  emitted by TN.

The molecular information rate achieved in the interval  $[t, t + \tau]$  in the deterministic point-to-point molecular channel, i.e.,  $R_p(t, \tau)$  (bits/ $\tau$  s), can be given as  $R_p(t, \tau) = n(t, \tau) - k(t, \tau)$ . However, since  $k(t, \tau)$  is a function of the channel input  $x$  as  $\lceil \frac{1}{2} \log h(t, \tau)x \rceil = k(t, \tau)$ ,  $R_p(t, \tau)$  is also a function of  $x$  such that  $R_p(t, \tau)$  decreases while  $x$  increases. This stems from the fact that in the channel model given in (10), the effect of the noise  $z$  increases with the factor  $[h(t, \tau)x]^{\frac{1}{2}}$  and the increasing noise effect reduces the molecular information rate. However, as introduced in Section 2,  $x$  has also a lower bound, i.e.,  $x_l$ , in order to obtain a coherent approximation for the channel output  $y(t, \tau)$ . Therefore, the maximum molecular information rate of the point-to-point molecular channel in the interval  $[t, t + \tau]$ , i.e.,  $R_p(t, \tau)$ , can be obtained by selecting the channel input  $x$  as its lower bound  $x_l$  and can be given as

$$R_p(t, \tau) = n(t, \tau) - k(t, \tau) = \lceil \log h(t, \tau) \rceil - \left\lceil \frac{1}{2} \log \left( h(t, \tau) \frac{x_l}{x_u} \right) \right\rceil. \quad (15)$$

Due to the extremely long propagation delay of the emitted molecules, the molecular information rate  $R_p(t, \tau)$  is a time-varying function. Here, in order to define an ultimate average capacity for the point-to-point molecular channel, starting from  $t_0 = 0$ , we simply average consecutive  $R_p(t, \tau)$  values computed during a sufficiently high number of consecutive intervals of  $\tau$ . For example, during  $T$  consecutive intervals of  $\tau$ , we have  $T$  molecular information rates as  $R_p(t_0, \tau)$ ,  $R_p(t_0 + \tau, \tau)$ ,  $R_p(t_0 + 2\tau, \tau)$ ,  $\dots$ ,  $R_p(t_0 + (T - 1)\tau, \tau)$  and the capacity achieved during these intervals can be obtained by averaging these rates. Hence, the average capacity of the point-to-point molecular channel, i.e.,  $\Pi$ , can be given as

$$\Pi = \frac{1}{T} \sum_{i=0}^{T-1} R_p(t_0 + i\tau, \tau). \quad (16)$$

In the point-to-point molecular channel, the molecular communication rate between TN and RN can be clearly increased with the channel gain  $h(t, \tau)$  on account of  $\lceil \log h(t, \tau) \rceil = n(t, \tau)$ . However, the channel gain  $h(t, \tau)$  is mostly affected by the physical system parameters such

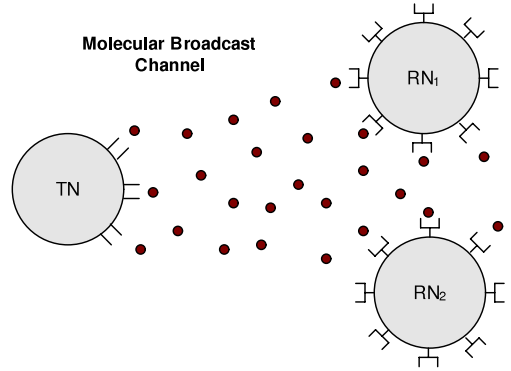


Fig. 3. Molecular broadcast channel with one TN simultaneously communicating with two RNs.

as diffusion coefficient and distance between nanomachines as introduced in Section 2. Therefore, the regulation of such physical parameters to improve the gain may not be always possible since these parameters are initially set and cannot be changed throughout. Similar to the traditional wireless communication, by increasing the upper bound of the channel input ( $x_u$ ), the channel gain  $h(t, \tau)$  and the capacity of point-to-point molecular channel can be increased. However,  $x_u$  may be also determined by the physical molecular emission capabilities of nanomachines. Hence, it might not be possible to improve  $x_u$  without the regulation of physical system parameters. On the other hand, since TN needs an energy resource to emit each of molecules  $L$ , there may be a rough trade off between energy consumption and the achievable capacity level. Thus, similar to traditional wireless communication, in a point-to-point molecular channel, the communication rate is clearly prone to an extremely low level of nanomachine energy resource.

### 3.2. Molecular broadcast channel

In the molecular broadcast channel, single TN communicates with multiple RNs as shown in Fig. 3. Based on the point-to-point molecular channel devised in Section 3.1, it is straightforward to find the achievable molecular communication rate in each RN for molecular broadcast channel. If we consider the case in which a single TN communicates with two RNs called as  $RN_1$  and  $RN_2$ , following the channel model given in (10), the channel output in

$RN_1$  and  $RN_2$ , i.e.,  $y_1(t, \tau)$  and  $y_2(t, \tau)$ , respectively, can be given as

$$\begin{aligned} y_1(t, \tau) &= h_1(t, \tau)x + [h_1(t, \tau)x]^{\frac{1}{2}}z \quad \text{and} \\ y_2(t, \tau) &= h_2(t, \tau)x + [h_2(t, \tau)x]^{\frac{1}{2}}z. \end{aligned} \quad (17)$$

Using the binary expansion of  $x$  and  $z$ , the channel outputs  $y_1(t, \tau)$  and  $y_2(t, \tau)$  can be expressed as

$$\begin{aligned} y_j(t, \tau) &= 2^{\log h_j(t, \tau)} \sum_{i=1}^{\infty} x(i)2^{-i} \\ &+ 2^{\frac{1}{2} \log h_j(t, \tau)x} \sum_{i=1}^{\infty} z(i)2^{-i}, \quad \text{for } j = 1, 2. \end{aligned} \quad (18)$$

In order to give a deterministic model for molecular broadcast channel, (18) can be simplified as

$$\begin{aligned} y_j(t, \tau) &\approx 2^{n_j(t, \tau)} \sum_{i=1}^{n_j(t, \tau) - k_j(t, \tau)} x(i)2^{-i} \\ &+ 2^{k_j(t, \tau)} \sum_{i=1}^{\infty} [x(i + n_j(t, \tau) - k_j(t, \tau)) + z(i)]2^{-i} \end{aligned}$$

for  $j = 1, 2$ , (19)

where  $\lceil \log h_j(t, \tau) \rceil = n_j(t, \tau)$  and  $\lceil \frac{1}{2} \log h_j(t, \tau)x \rceil = k_j(t, \tau)$  for  $j = 1, 2$ . Based on the deterministic model given in (19), the molecular communication rate between TN and  $RN_j$  in the time interval  $[t, t + \tau]$ , i.e.,  $R_b^j(t, \tau)$  for  $j = 1, 2$ , can be given as

$$\begin{aligned} R_b^j(t, \tau) &= n_j(t, \tau) - k_j(t, \tau) \\ &= \lceil \log h_j(t, \tau) \rceil - \left\lceil \frac{1}{2} \log \left( h_j(t, \tau) \frac{x_l}{x_u} \right) \right\rceil \end{aligned}$$

for  $j = 1, 2$ . (20)

Here, similar to the point-to-point molecular channel, by averaging the molecular communication rates obtained during  $T$  consecutive intervals of  $\tau$ , average capacity achieved by each  $RN_j$ , i.e.,  $A_j$  can be given as

$$A_j = \frac{1}{T} \sum_{i=0}^{T-1} R_b^j(t_0 + i\tau, \tau) \quad \text{for } j = 1, 2. \quad (21)$$

Due to free diffusion of the emitted molecules in all directions, unicast and multicast routing among nanomachines may not be feasible in molecular communication. Therefore, the molecular broadcast channel is indispensable for molecular nanonetworks to provide an efficient flooding-based routing scheme among nanomachines. In fact, due to the free diffusion of emitted molecules, each molecular transmission can ultimately reach all nanomachines in the system. This imposes a high level of molecular interference on the nanonetwork. Therefore, it is essential for an efficient routing mechanism to choose a set of broadcaster nanomachines to efficiently route molecular information from a source to a destination nanomachine by imposing the minimum level of molecular interference on the other nanomachines.

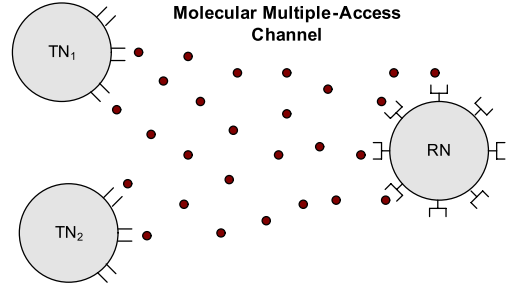


Fig. 4. Molecular multiple-access channel with two TNs simultaneously communicating with a single RN.

### 3.3. Molecular multiple-access channel

In the molecular multiple-access channel, multiple TNs communicate with a single RN. Therefore, a single RN simultaneously receives multiple molecular transmissions from all TNs. Here, we consider a molecular multiple-access channel in which two TNs ( $TN_1$  and  $TN_2$ ) communicate with a single RN as shown in Fig. 4. The molecular communication channel model given in (10) also has a useful characteristic based on which molecular multiple-access channel can also be modeled using (10). This follows the fact that the superposition of Poisson random variables is also a Poisson random variable, the rate of which is the sum of the rates of all Poisson random variables. Let us assume that two TNs called  $TN_1$  and  $TN_2$  transmit to a single RN in a molecular multiple-access channel and each  $TN_i$  has the channel gain  $h_i(t, \tau)$  and channel input  $x_i$  for  $i = 1, 2$ . Let us also assume that  $x_i$  has a lower and upper bound given as  $x_l^i$  and  $x_u^i$ , respectively, for  $i = 1, 2$ . Hence, the channel output  $y(t, \tau)$  of the molecular multiple-access channel can be given as

$$\begin{aligned} y(t, \tau) &= h_1(t, \tau)x_1 + h_2(t, \tau)x_2 \\ &+ [h_1(t, \tau)x_1 + h_2(t, \tau)x_2]^{\frac{1}{2}}z, \end{aligned} \quad (22)$$

(22) clearly leads to a realistic channel model for molecular multiple-access channel. Using the binary expansion of  $x_1$ ,  $x_2$ , and  $z$ , (22) can be also expressed as

$$\begin{aligned} y(t, \tau) &= 2^{\log h_1(t, \tau)} \sum_{i=1}^{\infty} x_1(i)2^{-i} + 2^{\log h_2(t, \tau)} \sum_{i=1}^{\infty} x_2(i)2^{-i} \\ &+ 2^{\frac{1}{2} \log [h_1(t, \tau)x_1 + h_2(t, \tau)x_2]} \sum_{i=1}^{\infty} z(i)2^{-i}. \end{aligned} \quad (23)$$

Simplifying (23), the deterministic model of the molecular multiple-access channel can be given as

$$\begin{aligned} y(t, \tau) &\approx 2^{n_1(t, \tau)} \sum_{i=1}^{n_1(t, \tau) - n_2(t, \tau)} x_1(i)2^{-i} \\ &+ 2^{n_2(t, \tau)} \sum_{i=1}^{n_2(t, \tau) - k(t, \tau)} \left[ x_1(i + n_1(t, \tau) - n_2(t, \tau)) \right. \\ &+ \left. x_2(i) \right] 2^{-i} + 2^{k(t, \tau)} \sum_{i=1}^{\infty} \left[ x_1(i + n_1(t, \tau) - k(t, \tau)) \right. \\ &+ \left. x_2(i + n_2(t, \tau) - k(t, \tau)) + z(i) \right] 2^{-i}, \end{aligned} \quad (24)$$

where  $n_j(t, \tau) = \lceil \log h_j(t, \tau) \rceil$  for  $j = 1, 2$  and  $k(t, \tau) = \lceil \frac{1}{2} \log(h_1(t, \tau)x_1 + h_2(t, \tau)x_2) \rceil$ . As seen in (24),  $[n_1(t, \tau) - n_2(t, \tau)]$  most significant bits of  $x_1$  can be received by RN without any noise and  $[n_2(t, \tau) - k(t, \tau)]$  bits of  $x_1$  and  $x_2$  interfere with each other. The other bits of  $x_1$  and  $x_2$  cannot be seen by RN since they interfere with the noise [16]. Similar to traditional wireless multiple-access channels, the molecular multiple-access channel is also prone to interference among TNs that simultaneously transmit to the same channel. In a traditional wireless multiple-access channel, the interference can be relieved by means of efficient multiple-access mechanisms such as code division multiple access (CDMA). However, in a molecular multiple-access channel, a coding mechanism that can separate the molecular transmissions in order not to interfere with each other may not be practical due to extremely low propagation speed of molecules and lack of synchronization among TNs. Instead, it may be possible to enable each TN to use different molecules as carriers that are distinguished by RN when they are perceived. This can clearly prevent a high interference level in the molecular multiple-access channel. Hence, if each TN uses a different molecule for a communication carrier the molecular communication rate achieved by TN<sub>1</sub> and TN<sub>2</sub> in the interval  $[t, t + \tau]$ , i.e.,  $R_m^1(t, \tau)$  and  $R_m^2(t, \tau)$ , respectively, can be given as

$$\begin{aligned} R_m^j(t, \tau) &= n_j(t, \tau) - k(t, \tau) \\ &= \left\lceil \log h_j(t, \tau) \right\rceil - \left\lceil \frac{1}{2} \log \left( h_1(t, \tau) \frac{x_1^1}{x_u^1} \right. \right. \\ &\quad \left. \left. + h_2(t, \tau) \frac{x_1^2}{x_u^2} \right) \right\rceil \quad \text{for } j = 1, 2. \end{aligned} \quad (25)$$

If such a multiple-access mechanism is not used, communication rate in the molecular multiple-access channel excessively decreases due to high interference level between  $x_1$  and  $x_2$ . More specifically, in this case, TN<sub>1</sub> achieves  $[n_1(t, \tau) - n_2(t, \tau)]$  bits of molecular communication rate while TN<sub>2</sub> may not use any capacity in the molecular multiple-access channel due to the excessive interference level. In order to obtain the average capacity, i.e.,  $\Gamma_j$  achieved by each TN in the molecular multiple-access channel, molecular communication rates  $R_m^j(t, \tau)$  measured along  $T$  consecutive intervals of  $\tau$  are averaged as follows

$$\Gamma_j = \frac{1}{T} \sum_{i=0}^{T-1} R_m^j(t_0 + i\tau, \tau) \quad \text{for } j = 1, 2. \quad (26)$$

Next, using the capacity expressions derived for molecular point-to-point, broadcast, and multiple-access channels, we investigate the deterministic capacity of information flow in a molecular nanonetwork.

### 3.4. Information flow in a molecular nanonetwork

Here, we investigate deterministic capacity of information flow between a source nanomachine  $S$  and a destination nanomachine  $D$  in a diamond-like molecular nanonetwork as shown in Fig. 5(a). We assume that  $S$  cannot directly communicate with  $D$  and two relay

nanomachines called as  $L_1$  and  $L_2$  help the molecular communication between  $S$  and  $D$ . We also assume that all nanomachines in the network have the capability of molecule emission and reception to transmit and receive the molecular information as a relay. The network consists of a molecular broadcast channel among  $S, L_1$ , and  $L_2$  and a molecular multiple-access channel among  $L_1, L_2$ , and  $D$ . These channels are schematically shown in Fig. 5(b) and achievable molecular communication rates within the interval  $[t, t + \tau]$  in these channels can be computed using the deterministic capacity expressions given in (20) and (25) in Sections 3.2 and 3.3.  $b_i(t, \tau)$  denotes the achievable molecular communication rate between  $S$  and  $L_i$  in the interval  $[t, t + \tau]$  for  $i = 1, 2$  and  $m_i(t, \tau)$  denotes the achievable rate between  $L_i$  and  $D$  in the interval  $[t, t + \tau]$  for  $i = 1, 2$ .

Here, we aim to find the capacity of maximum information flow between  $S$  and  $D$  using the maximum-flow minimum cut theorem [17]. We first focus on the time interval  $[t, t + \tau]$  to find the achievable molecular communication rate in this interval. Then, we average the rates obtained along a sufficiently high number of consecutive intervals of  $\tau$  to find the average capacity of the information flow between  $S$  and  $D$ . As observed in Fig. 5(b), there are four cut sets, i.e.,  $\xi_i, i = 1, \dots, 4$ , in the diamond-like molecular nanonetwork [16]. The first cut set, i.e.,  $\xi_1 = \{(S, L_1), (S, L_2)\}$  forms a broadcast channel among  $S, L_1$ , and  $L_2$ . Based on the deterministic capacity analysis of molecular broadcast channel given in Section 3.2, the achievable molecular communication rate within the interval  $[t, t + \tau]$  in the first cut set can be given as  $\max(b_1(t, \tau), b_2(t, \tau))$ . The second cut set, i.e.,  $\xi_2 = \{(L_1, D), (L_2, D)\}$  forms a molecular multiple-access channel among  $L_1, L_2$ , and  $D$ . Using the deterministic capacity of the molecular multiple-access channel given in Section 3.3, the molecular communication rate achieved during the interval  $[t, t + \tau]$  in this cut set can be given as  $\max(m_1(t, \tau), m_2(t, \tau))$ . The third cut set, i.e.,  $\xi_3 = \{(S, L_1), (L_2, D)\}$  consists of two molecular communication links and the molecular rate in this set can be given as  $(b_1(t, \tau) + m_2(t, \tau))$ . The last cut set, i.e.,  $\xi_4 = \{(S, L_2), (L_1, D)\}$ , also consists of two molecular communication links and the molecular information rate in this set can be given as  $(b_2(t, \tau) + m_1(t, \tau))$ . According to the maximum-flow minimum cut theorem [17], capacity of information flow between  $S$  and  $D$  during the interval  $[t, t + \tau]$ , i.e.,  $R_d(t, \tau)$  is equal to the minimum cut set capacity in the molecular nanonetwork shown in Fig. 5 and can be given as [16]

$$\begin{aligned} R_d(t, \tau) &= \min[\max(b_1(t, \tau), b_2(t, \tau)), \\ &\quad \max(m_1(t, \tau), m_2(t, \tau)), (b_1(t, \tau) \\ &\quad + m_2(t, \tau)), (b_2(t, \tau) + m_1(t, \tau))]. \end{aligned} \quad (27)$$

The average capacity of information flow, i.e.,  $\Phi$ , can be obtained by averaging  $R_d(t, \tau)$  values observed in  $T$  number of consecutive intervals of  $\tau$  as

$$\Phi = \frac{1}{T} \sum_{i=0}^{T-1} R_d(t_0 + i\tau, \tau). \quad (28)$$

The capacity analysis of information flow between  $S$  and  $D$  reveals that in a molecular nanonetwork, routing





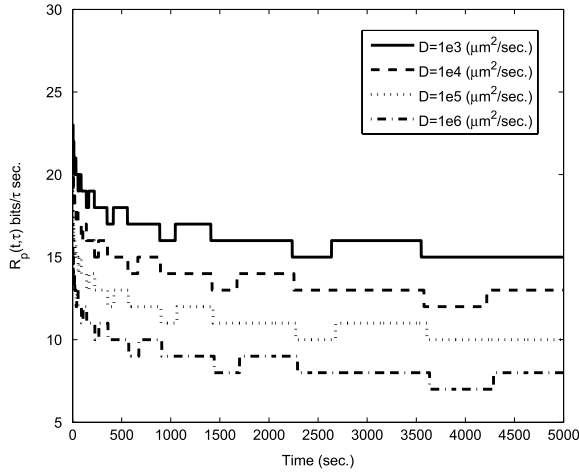


**Fig. 7.** Information rate of point-to-point molecular channel for the different diffusion coefficients of the medium with time.

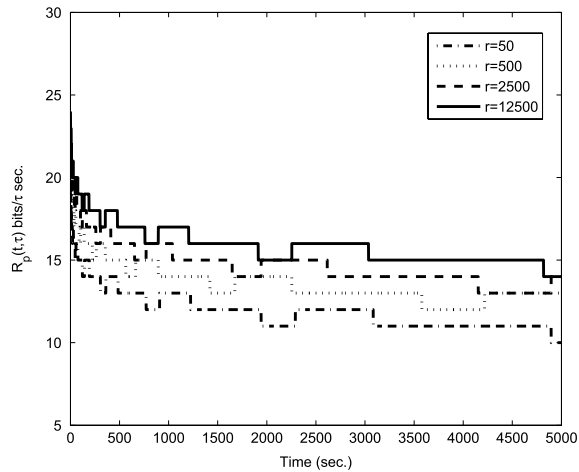


**Fig. 8.** Information rate of point-to-point molecular channel for the different receptor concentration with time.

In Fig. 7,  $R_p(t, \tau)$  is shown for different diffusion coefficients  $D$  ( $\mu\text{m}^2/\text{s}$ ). The diffusion coefficient is a major parameter for the molecular information rate since it determines the average number of molecules that react with the receptors in VRV during the time interval  $[t, t + \tau]$ . As the diffusion coefficient increases,  $R_p(t, \tau)$  also decreases. When the molecules are initially emitted by TN, the molecules diffuse in the medium and immediately reach to close proximity of RN and react with the receptors in VRV. After a course of time, the number of molecules in VRV starts to decrease since the molecules continue to diffuse in all directions to which they do not reach yet. This decreases the molecule concentration in VRV and also decreases  $R_p(t, \tau)$  with time. Hence, as the diffusion coefficient increases, the number of molecules in VRV decreases more quickly and the molecular communication rate decreases as shown in Fig. 7.

In Fig. 8, we observe the effect of receptor concentration ( $r$ ) on the information rate of point-to-point molecular channel ( $R_p(t, \tau)$ ). Similar to the diffusion coefficient,  $r$  also determines the reaction rate between the molecules

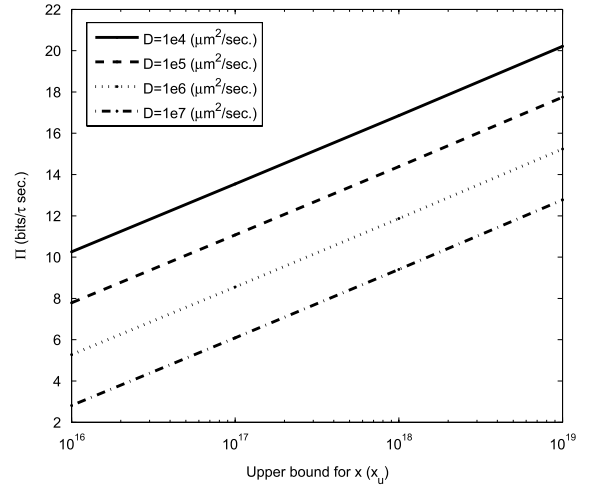


**Fig. 9.** Average capacity of point-to-point molecular channel according to varying  $x_u$  with different  $D$  values.

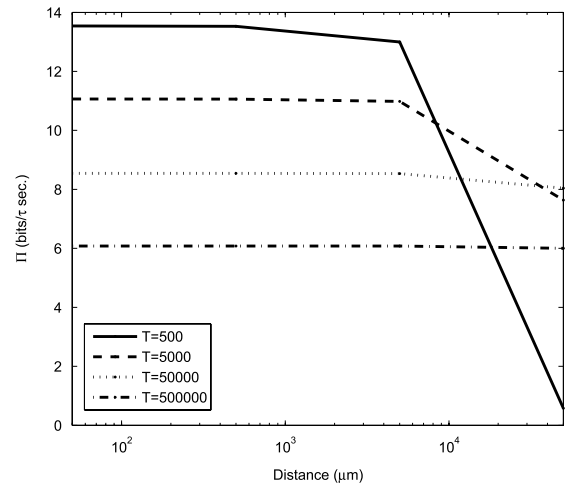


**Fig. 10.** Average capacity of point-to-point molecular channel according to varying internode distance ( $d$ ) with different observation intervals ( $T$ ).

and receptors in VRV such that  $R_p(t, \tau)$  increases with  $r$ . However, due to continuous diffusion of molecules, the molecule concentration in VRV decreases with time and the rate also decreases regardless of the receptor concentration as in Fig. 8.

The average capacity  $\Pi$  is also shown in Fig. 9 according to the different diffusion coefficient levels with increasing  $x_u$ . Fig. 9 clearly follows the results observed in Figs. 6 and 7 since  $\Pi$  is obtained by simply averaging  $R_p(t, \tau)$  values observed in  $T$  consecutive intervals of  $\tau$ .  $\Pi$  increases with  $x_u$ , which is also shown in Fig. 6. Moreover, as the diffusion coefficient  $D$  increases,  $\Pi$  decreases. This result can also be seen in Fig. 7. In Fig. 10,  $\Pi$  is shown according to different distances between TN and RN with varying observation intervals  $T$ . For the lowest level of observation interval, i.e.,  $T = 500$ , the molecules cannot completely reach to the longest distance, i.e.,  $d = 5e4 \mu\text{m}$  at the last of the  $T = 500$  intervals. This results in an extreme reduction in  $\Pi$ . However, as  $T$  increases, the molecules easily reach

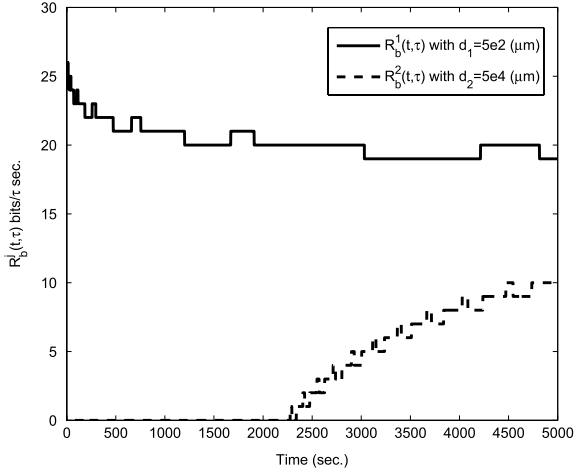


**Fig. 11.** Information rate achieved by two distinct RNs located to different distances from a single TN in a molecular broadcast channel.

to the long distances and provide high level of molecular communication capacity. On the other hand, as  $T$  increases, due to the continuous diffusion of the molecules, the capacity decreases with time and consequently, average capacity becomes low for higher  $T$  values.

#### 4.2. Molecular broadcast channel

Here, we observe the molecular information rate in a molecular broadcast channel. Due to the fact that molecular communication is based on the free diffusion of molecules toward all directions, the molecular broadcast channel has similar characteristics with the point-to-point molecular channel. Especially, the effects of  $x_u$ ,  $D$ , and  $r$  are the same as the point-to-point molecular channel. However, if RNs have different channel gains due to their different distances to TN, the molecular broadcast channel may provide varying rate levels in two RNs, i.e., RN<sub>1</sub> and RN<sub>2</sub>. In Fig. 11, we show the molecular information rate ( $R_b^j(t, \tau)$ ) within the interval  $[t, t + \tau]$  in the molecular broadcast channel with a single TN and RN <sub>$j$</sub>  for  $j = 1, 2$ . We assume that the distances from TN to RN<sub>1</sub> and RN<sub>2</sub> are different and given as  $d_1 = 5e2 \mu\text{m}$  and  $d_2 = 5e4 \mu\text{m}$ , respectively. Due to  $d_1 < d_2$ , the emitted molecules reach to RN<sub>2</sub> later than RN<sub>1</sub>. As observed in Fig. 11, until  $t = 2300$  s, RN<sub>2</sub> does not receive any molecule in its VRV although RN<sub>1</sub> already experiences many reactions. Hence, internode distances are the main determinant for the molecular information rate experienced by RN <sub>$j$</sub>  in a molecular broadcast channel.

#### 4.3. Molecular multiple-access channel

Similar to the traditional wireless multiple-access channel, the most critical barrier toward the realization of molecular multiple-access communication is the interference among the transmitter nanomachines that simultaneously access to the same receiver nanomachine. However, unlike the traditional multiple access mechanisms such as code division multiple access (CDMA) and time division multiple access (TDMA), in the molecular multiple-access

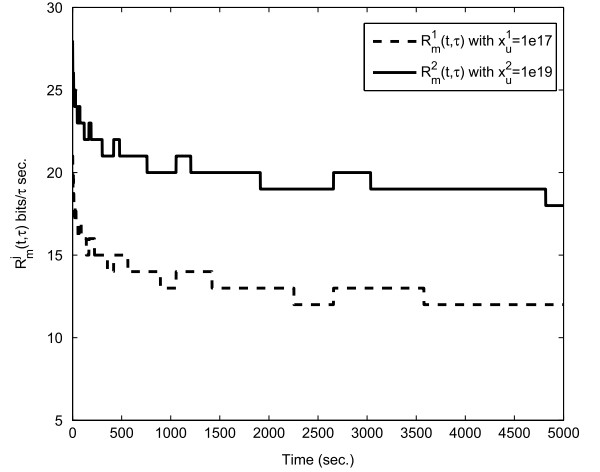


**Fig. 12.** Information rate achieved by two distinct TNs using different level of upper bound for channel input to access a single RN.

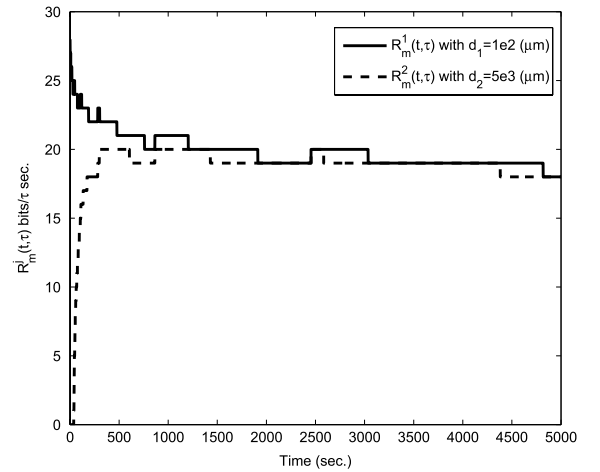


**Fig. 13.** Information rate achieved by two TNs located in different distances from RN in a molecular multiple-access channel.

channel, the interference among the transmitter nanomachines can be prevented by enabling each TN to use different kinds of molecule that can be uniquely distinguished by RN. In Fig. 12, the molecular information rates,  $R_m^j(t, \tau)$ , achieved by TN<sub>1</sub> and TN<sub>2</sub> with  $x_u^1 = 1e17$  and  $x_u^2 = 1e19$ , respectively, are illustrated.

Clearly, TN<sub>2</sub> reaches a rate higher than TN<sub>1</sub> since  $x_u^2 > x_u^1$ . In Fig. 13,  $R_m^j(t, \tau)$  achieved by each of two distinct TNs located at different distances from a single RN is shown for  $j = 1, 2$ . Similar to the molecular broadcast channel, in the molecular multiple-access channel, the transmission distance strongly affects the molecular information rate. The distances from RN to TN<sub>1</sub> and TN<sub>2</sub>, i.e.,  $d_1$  and  $d_2$ , respectively, are given as  $d_1 = 1e2 \mu\text{m}$  and  $d_2 = 5e3 \mu\text{m}$ . Clearly, as  $d_1 < d_2$ , the molecules emitted by TN<sub>1</sub> reach to RN more quickly than the other molecules emitted by TN<sub>2</sub>. Therefore, TN<sub>1</sub> quickly experiences a higher molecular communication rate and as the emitted molecules diffuse this decreases the average number of molecules in VRV and the molecular communication rate decreases. Conversely,

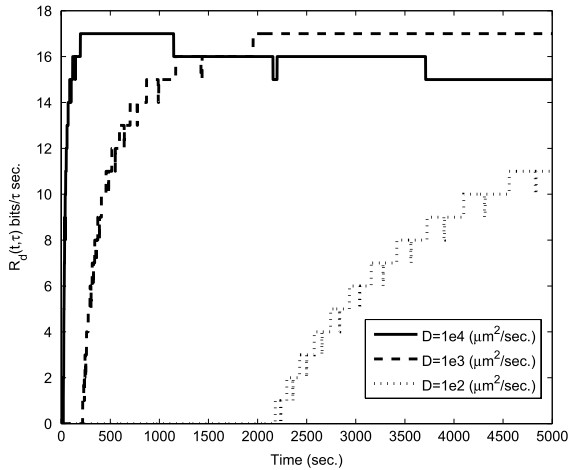


**Fig. 14.** Information flow capacity in diamond-like molecular nanonetwork for different diffusion coefficients.

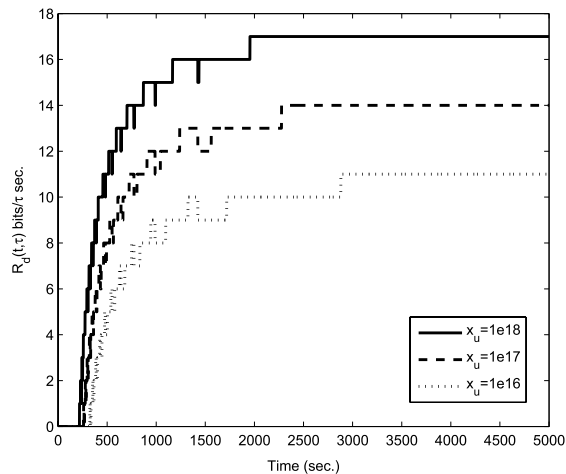


**Fig. 15.** Information flow capacity in diamond-like molecular nanonetwork for different upper bound levels of channel inputs.

since the distance between  $TN_2$  and  $RN$  is higher, the molecules emitted by  $TN_2$  reach to  $VRV$  of  $RN$  later than the other molecules emitted by  $TN_2$ . Thus,  $TN_2$  communicates with  $RN$  after its molecules reach to  $VRV$  of  $RN$  and the rate abruptly increases. After a course of time,  $TN_1$  and  $TN_2$  start to achieve the same information rate level.

#### 4.4. Diamond-like molecular nanonetwork

The diamond-like molecular nanonetwork consists of a molecular broadcast and multiple-access channel. Therefore, the capacity of information flow between a source and destination nanomachines is affected by the characteristics of these channels. Here, we observe the effects of  $D$  and  $x_u$  on the information flow rate in the diamond-like molecular nanonetwork. In Fig. 14, the information flow rate is shown according to different  $D$ . Contrary to the point-to-point molecular channel, as

$D$  increases, the information flow rate also increases. Moreover, due to the low level of diffusion coefficient that results in high propagation delay, the rate becomes 0 during a time interval. However, as soon as the molecules reach to the  $VRV$  of the destination nanomachine, it abruptly increases. In Fig. 15, we observe the effect of  $x_u$  on the information flow capacity. As observed, similar to the point-to-point molecular channel, as  $x_u$  increases, the information flow rate increases in the diamond-like molecular nanonetworks.

## 5. Conclusion

In this paper, using the stochastic models in chemically reacting systems, we first devise a realistic channel model for molecular communication. Then, we define and analyze the molecular point-to-point, broadcast, and multiple-access channels. We also investigate the deterministic capacity of information flow in a molecular nanonetwork. Our models and investigations clearly reveal that molecular communication links among nanomachines can be established with sufficiently high communication rate in nanonetworks. Unlike the traditional Gaussian communication channel, in the molecular communication channel achievable capacity is affected by the both the lower and upper bound of the channel input. This arises from the input-dependent noise term. In the point-to-point and broadcast molecular communication channel, communication rate can be improved by increasing the upper bound of the channel input. However, there is a rough trade-off between communication rate and energy consumption of nanomachines. In the molecular multiple-access channel, in order to obtain a sufficiently high molecular communication rate, transmitter nanomachines must either schedule their transmissions or use different kinds of molecule that are distinguished by the receiver nanomachines. Due to the very low-end computation and synchronization capabilities of nanomachines, it may not be possible for transmitter nanomachines to schedule their transmissions. Instead, the transmitter nanomachines may use different kinds of molecules to obtain a sufficient level of molecular communication rate. In a molecular nanonetwork, it may be possible to communicate with the network nodes that cannot directly communicate with each other with the help of relay nodes with a satisfactorily high communication rate. This may allow a possible realization of a routing scheme in a molecular nanonetwork, which needs to be further investigated.

## Acknowledgements

This work was supported in part by the Turkish Scientific and Technical Research Council under Grant no. #109E257 and by the Turkish National Academy of Sciences Distinguished Young Scientist Award Program (TUBA-GEBIP).

## References

- [1] E. Drexler, *Engines of creation: the coming era of nanotechnology*, Doubleday, New York, 1986.
- [2] I.F. Akyildiz, F. Brunetti, C. Blazquez, *NanoNetworking: a new communication paradigm*, *Computer Networks Journal* (Elsevier) (June) (2008).
- [3] R.A. Freitas, *Nanomedicine, Volume I: Basic capabilities*, Landes Bioscience, Texas, USA, 1999.
- [4] T Suda, M Moore, T Nakano, R Egashira, A Enomoto, *Exploratory research on molecular communication between nanomachines*. In: *Proc. GECCO 2005*. 2005.
- [5] S Hiyama, Y Isogawa, T Suda, Y Moritani, K Sutoh, *A design of an autonomous molecule loading/transporting/unloading system using DNA hybridization and biomolecular linear motors*. In: *Proc. European nano systems 2005*. 2005.
- [6] M Pierobon, IF Akyildiz, *A physical end-to-end model for molecular communication in nanonetworks*, *IEEE Journal on Selected Areas in Communications* 28 (4) (2010) 602–611.
- [7] AW Eckford, *Molecular communication: physically realistic models and achievable information rates*. *IEEE Transactions on Information Theory*. 2008 [submitted for publication]. Available in arXiv.
- [8] B. Atakan, O.B. Akan, *On channel capacity and error compensation in molecular communication*, *Springer Transactions on Computational System Biology* 10 (February) (2008) 59–80.
- [9] B Atakan, OB Akan, *On molecular multiple-access, broadcast and relay channels in nanonetworks*. In: *Proc. ACM BIONETICS 2008*. 2008.
- [10] B Atakan, OB Akan, *Single and multiple-access channel capacity in molecular nanonetworks*. In: *Proc. ICST/ACM Nano-Net 2009*. 2009.
- [11] D.T. Gillespie, *Exact stochastic simulation of coupled chemical reactions*, *Journal of Physical Chemistry* 81 (25) (1977) 2340–2361.
- [12] H.C. Berg, E.M. Purcell, *Physics of chemoreception*, *Biophysical Journal* 20 (2) (1977) 193–219.
- [13] T.E. Turner, S. Schnell, K. Burrage, *Stochastic approaches for modelling in vivo reactions*, *Computational Biology and Chemistry* (Elsevier) 28 (3) (2004) 165–178.
- [14] D.T. Gillespie, *The chemical Langevin equation*, *Journal of Chemical Physics* 113 (1) (2000) 297–306.
- [15] D.T. Gillespie, *Markov processes: an introduction for physical scientists*, Academic, San Diego, 1992.
- [16] S Avestimehr, S Diggavi, D Tse, *A deterministic approach to wireless relay networks*. In: *Allerton conference*. 2007.
- [17] L.R. Ford, D.R. Fulkerson, *Flows in networks*, Princeton University Press, New Jersey, Princeton, 1962.



**Baris Atakan** received B.Sc. and M.Sc. degrees in Electrical and Electronics Engineering from Ankara University and Middle East Technical University, Ankara, Turkey, in 2000 and 2005, respectively. He is currently a research assistant in the Next-generation Wireless Communication Laboratory and pursuing his Ph.D. degree at the Department of Electrical and Electronics Engineering, Middle East Technical University. His current research interests include nanoscale communication, and biologically-inspired communication protocols for wireless sensor networks and cognitive radio networks.



**Ozgun B. Akan** received B.Sc. and M.Sc. degrees in Electrical and Electronics Engineering from Bilkent University and Middle East Technical University, Ankara, Turkey, in 1999 and 2001, respectively. He received a Ph.D. in electrical and computer engineering from the Broadband and Wireless Networking Laboratory, School of Electrical and Computer Engineering, Georgia Institute of Technology, Atlanta, in 2004. He is currently Associate Professor with the Department of Electrical and Electronics Engineering, Middle East Technical University and the Director of Next-generation Wireless Communications Laboratory (NWCL). His current research interests are in wireless communications, bio-inspired communications, nanoscale and molecular communications, network information theory.

Dr. Akan is an Associate Editor for *IEEE Transactions on Vehicular Technology*, Editor for *Nano Communication Networks Journal* (Elsevier), *ACM/Springer Wireless Networks (WINET) Journal*, *International Journal of Communication Systems* (Wiley). He served as an Area Editor for *AD HOC Networks Journal* (Elsevier) (between 2004–2008), as a Guest Editor for several special issues, as the General Co-Chair for The Third International Conference on Bio-Inspired Models of Network, Information, and Computing Systems (ICST/IEEE BIONETICS 2008), the European Vice Chair for The Second International Conference on Nano-Networks (ICST/ACM Nano-Net 2007), an International Vice Chair for IEEE INFOCOM 2006, and in organizing committees and technical program committees of many other international conferences. He is the Vice President for the IEEE Communications Society – Turkey Section. He is an IEEE Senior Member (Communications Society), and a member of ACM. Dr. Akan received the IBM Faculty Award 2008, Turkish Academy of Sciences Distinguished Young Scientist Award 2008 (TUBA-GEBIP).